INTERNATIONAL JOURNAL FOR NUMERICAL METHODS IN FLUIDS
Int. J. Numer. Meth. Fluids 2004; **44**:861–884 (DOI: 10.1002/fld.678)

Review of numerical special relativistic hydrodynamics

D. E. A. van Odyck*,†

CWI, P.O. Box 94079, 1090 GB Amsterdam, The Netherlands

SUMMARY

This paper gives an overview of numerical methods for special relativistic hydrodynamics (SRHD). First, a short summary of special relativity is given. Next, the SRHD equations are introduced. The exact solution for the SRHD Riemann problem is described. This solution is used in a Godunov scheme to compute solutions for two test problems. A third test problem is used to show non-convergent behaviour of the numerical solution at the location of the contact discontinuity. Finally, a short description of numerical methods used so far in SRHD is given. Copyright © 2004 John Wiley & Sons, Ltd.

KEY WORDS: special relativity; hydrodynamics; Riemann problems

1. INTRODUCTION

The Euler equations are not adequate to describe a fluid flowing with nearly the speed of light. A relativistic approach is needed to model such high-speed fluids. Fluids flowing with relativistic speeds are encountered in astrophysics. Relativistic jets (resulting from accretion onto compact objects) and gamma-ray bursts (GRBs, high-energy explosions of not yet determined objects in the universe, at cosmological distances from the earth) can be modelled with the use of special relativistic hydrodynamics. Simulations of relativistic jets have been performed by Aloy *et al.* [1] and of GRBs by Piran *et al.* [2]. Also, in the field of heavy-ion collisions special relativistic hydrodynamics can be applied, see Reference [3]. The ions are then modelled as droplets of fluid whose properties are governed by a nuclear equation of state. This article gives a review of and an introduction to SRHD and shows that for a certain test problem non-convergent behavior of the numerical solution can occur. In a forthcoming article [4] these numerical problems are studied in more detail.

*Correspondence to: D. E. A. van Odyck, Bronckhorststraat 37-1, 1071 WP, Amsterdam, The Netherlands.
†E-mail: D.E.A.van.Odyck@cwi.nl

Contract/grant sponsor: Research supported by the Netherlands Organization for Scientific Research (NWO); contract/grant number: 635.000.003

Received 25 February 2003
Revised 31 August 2003

In the following an introduction to special relativity is given. We closely follow the book of D'Inverno [5]. The frame of reference from which an event is observed is a key ingredient in the theory of special relativity. The following terminology is frequently used:

- Inertial system: linearly moving frame of reference.
- Laboratory frame: frame of reference in which 'experiments' are observed.
- Rest frame: frame of reference connected to a particle or fluid element.

Einstein puts forward two postulates from which he develops special relativity.

Postulate 1
Principle of special relativity: all inertial observers are equivalent.

Postulate 2
Constancy of the speed of light: the speed of light is the same in all inertial systems.

From these two postulates the theory of special relativity can be developed. Assume two inertial systems S and S'. They move with respect to each other at a relative speed v. A linear motion of a point particle with constant velocity will be seen by observers in both S and S' as a straight line in their co-ordinate system. It follows that a transformation between both co-ordinate systems is linear and only depends on the speed v. In the above reasoning the first postulate is used. The transformation between two inertial systems moving parallel to each other (the x-axis is aligned) is described by

$$\begin{pmatrix} t' \\ x' \\ y' \\ z' \end{pmatrix} = L \begin{pmatrix} t \\ x \\ y \\ z \end{pmatrix} \tag{1}$$

where L is a function of v only. It is assumed that space is isotropic, meaning there is no preferred direction in space, so $y' = y$ and $z' = z$.

At the moment the origins of S and S' pass each other, the clocks in both systems are synchronized and at the same time a light signal is emitted. In system S the light's wave front can be described by $I(t, \mathbf{x}) = 0$, where

$$I = x^2 + y^2 + z^2 - c^2 t^2 \tag{2}$$

In S' the same wave front can be seen and is described by $I'(t', \mathbf{x}') = 0$, where

$$I' = x'^2 + y'^2 + z'^2 - c^2 t'^2 \tag{3}$$

In the last equation the second postulate is used, the speed of light is the same in every inertial system. After a co-ordinate transformation the wave front $I = 0$ is described by $I' = 0$ in the S'-system. From this it follows that $I = aI'$, where a only depends on the absolute value of v.[‡] If we start from system S' it follows that $I' = aI$. So, $a = \pm 1$. Since for $v \to 0$

[‡]Cannot depend on the direction of v because that would contradict the isotropy of space. And a cannot depend on space and time co-ordinates either because that would contradict with the homogeneity of space and time.

we get $I \rightarrow I'$, it holds $a = 1$. We can therefore write

$$x^2 - c^2t^2 = x'^2 - c^2t'^2 \tag{4}$$

To solve this equation the following co-ordinate transformation is introduced

$$T = \mathrm{i}ct, \quad T' = \mathrm{i}ct', \quad \mathrm{i} = \sqrt{-1} \tag{5}$$

which transforms Equation (4) into

$$x^2 + T^2 = x'^2 + T'^2 \tag{6}$$

So, rotations in the (x, T)-space are solutions of Equation (6):

$$\begin{aligned} x' &= x \cos\theta + T \sin\theta \\ T' &= -x \sin\theta + T \cos\theta \end{aligned} \tag{7}$$

In S the origin of S' is at $x = vt$ and in S' it is at $x' = 0$. It now follows from (7) that $\tan\theta = \mathrm{i}v/c$ and after defining the factor

$$\beta = \frac{1}{\sqrt{(1 - v^2/c^2)}} \tag{8}$$

the so-called Lorentz transformation can be solved from (7):

$$\begin{pmatrix} t' \\ x' \\ y' \\ z' \end{pmatrix} = \begin{pmatrix} \beta(t - vx/c^2) \\ \beta(x - vt) \\ y \\ z \end{pmatrix} \tag{9}$$

A general Lorentz transformation can be found by first rotating the x-axis of the S-system parallel to the Lorentz boost direction, then performing a Lorentz boost and finally rotating back to the original direction. A rotation does not introduce new physics.

The Lorentz transformation introduces two interesting effects: length contraction and time dilation. Consider a rod that is moving parallel to the x-axis with speed v. In the reference frame moving with the rod, the rod's length is defined as $\Delta x' = x'_2 - x'_1$. After substitution of the Lorentz transformation it is found that

$$\Delta x' = \beta(x_2 - vt) - \beta(x_1 - vt) = \beta(x_2 - x_1) = \beta\Delta x \tag{10}$$

For the observer in the unprimed system at rest the rod is shortened by a factor $\sqrt{1 - v^2/c^2}$. Next, consider time dilation. With respect to an inertial system S a clock is moving with speed v. In the clock's frame S', the clock is placed at the origin, $x'_1 = x'_2 = 0$. Then a time difference in S can be coupled to a time difference in S':

$$\Delta t = t_2 - t_1 = \beta(t'_2 + vx'_2/c^2) - \beta(t'_1 + vx'_1/c^2) = \beta(t'_2 - t'_1) = \beta\Delta t' \tag{11}$$

The time in a moving system is always the shortest time. We conclude with a summary of Lorentz transformation properties:

- A Lorentz transformation in the x-direction is equivalent to a rotation in (x, T)-space.
- If $v \ll c$ then the Galilean transformation is retrieved: $t' = t$ and $x' = x - vt$.
- The inverse transformation is found by interchanging primed and unprimed variables and putting $v \rightarrow -v$.
- Length contraction: $\Delta x' = \beta \Delta x$.
- Time dilation: $\Delta t = \beta \Delta t'$.
- Two Lorentz transformations in for example the x-direction, a boost with v followed by a boost with v', can be combined into one. This is clear if a Lorentz transformation is represented by a rotation in (x, T)-space: $\theta'' = \theta' + \theta$. From trigonometry it is known that

$$\tan(\theta + \theta') = \frac{\tan\,\theta + \tan\,\theta'}{1 - \tan\,\theta \tan\,\theta'} \tag{12}$$

  from which it follows that

$$v'' = \frac{v + v'}{1 + vv'/c^2} \tag{13}$$

  This formula shows how to add velocities in the correct relativistic manner.
- The four-dimensional line element $(\mathrm{d}s)^2 = c^2(\mathrm{d}t)^2 - (\mathrm{d}x)^2 - (\mathrm{d}y)^2 - (\mathrm{d}z)^2$ is invariant under a Lorentz transformation.

In the following some aspects of relativistic mechanics are treated.

1.1. Relativistic mass

Assume the mass of a moving particle depends on its velocity just as the foregoing transformation between inertial systems is velocity dependent. Then consider the inelastic collision of two particles with masses m_1 and m_2 and with the same rest mass m_r. The mass m_1 is moving with velocity u along the x-axis and m_2 is at rest in the frame S. After the inelastic collision the resulting particle has mass M and speed U. In the centre-of-mass frame S' both particles move with the speed U in opposite directions. Conservation of mass and linear momentum in the S-frame results in

$$\begin{aligned} m_1(u) + m_\mathrm{r} &= M(U) \\ m_1(u)u + 0 &= M(U)U \end{aligned} \tag{14}$$

In the system S' the mass m_1 moves with speed U before the collision. Since the S'-system moves with a speed U relative to the laboratory frame S, the speed u of mass m_1 in the S-system can be found by the relativistic formula (13) for adding velocities:

$$u = \frac{2U}{1 + U^2/c^2} \tag{15}$$

From Equation (14) an expression for $m_1(u)$ can be found and from Equation (15) an expression for U can be found. Combining these two expressions gives for the mass of a particle

in motion with respect to the laboratory frame:

$$m_1(u) = \frac{m_r}{\sqrt{(1 - u^2/c^2)}} = \Gamma m_r \tag{16}$$

Note the difference between β in Equation (9) and the Lorentz factor Γ in Equation (16); $\beta = \beta(v)$ with v the relative velocity of two *inertial systems*, and $\Gamma = \Gamma(u)$ with u the velocity of a particle relative to the laboratory frame.

1.2. Relativistic energy

Expanding the expression for relativistic mass in terms of u/c gives

$$\begin{aligned} mc^2 &= m_r c^2 + \frac{1}{2} m_r u^2 + O\left(\frac{u^4}{c^2}\right) \\ &= \text{constant} + \text{kinetic energy} + \text{higher-order terms} \end{aligned} \tag{17}$$

This shows that relativistic mass contains the kinetic energy term of the particle. It can be shown that the conservation of relativistic mass leads to the conservation of kinetic energy in the Newtonian limit $u \ll c$. It can also be shown that the conservation of linear momentum with relativistic mass leads to the conservation of linear momentum in the Newtonian limit $u \ll c$. It is therefore put forward that in general a particle can be described by its energy and momentum according to

$$E = mc^2, \ \mathbf{p} = m\mathbf{u} \text{ with } m = \Gamma m_r \text{ and } \mathbf{u} = \frac{\mathrm{d}\mathbf{x}}{\mathrm{d}t} \tag{18}$$

After a little of algebra it can be shown that

$$(E/c)^2 - p_x^2 - p_y^2 - p_z^2 = m_r c^2 \tag{19}$$

This quantity is invariant under a Lorentz transformation because m_r is the same in all inertial systems.

1.3. Tensor calculus

It is clear from the above that time and space are connected to each other just like momentum and energy. To have a more compact way of writing things down in special relativity the Minkowski co-ordinate system is introduced. For this we need tensor formalism. An n-dimensional manifold is defined as a collection of points with co-ordinates $(x^1, \ldots, x^n)$.[§] Locally, a manifold corresponds to the Euclidean space. A tensor is an object defined on the manifold. A co-ordinate transformation is introduced because it is not always possible to describe the whole manifold in terms of one co-ordinate system. Consider the following co-ordinate transformation:

$$x'^{\alpha} = x'^{\alpha}(x^1, \ldots, x^n) = x'^{\alpha}(x) \tag{20}$$

[§]An example of a manifold is the collection of points on the surface of a sphere.

If the determinant of the Jacobian of this transformation

$$J' = \left| \frac{\partial x'^{\alpha}}{\partial x^{\beta}} \right| \tag{21}$$

is non-zero the inverse transformation exists:

$$x^{\alpha} = x^{\alpha}(x') \tag{22}$$

A tensor of rank (n, m) is an object defined on a manifold that transforms like:

$$T'^{\alpha_1 \cdots \alpha_n}_{\beta_1 \cdots \beta_m} = \frac{\partial x'^{\alpha_1}}{\partial x^{\gamma_1}} \cdots \frac{\partial x'^{\alpha_n}}{\partial x^{\gamma_n}} \frac{\partial x^{\lambda_1}}{\partial x'^{\beta_1}} \cdots \frac{\partial x^{\lambda_m}}{\partial x'^{\beta_m}} T^{\gamma_1 \cdots \gamma_n}_{\lambda_1 \cdots \lambda_m} \tag{23}$$

A scalar transforms like

$$\phi'(x') = \phi(x) \tag{24}$$

Unfortunately, the partial differentiation of a tensor does not result in a tensor. After the introduction of the affine connection $\Gamma^{\alpha}_{\beta\lambda}$ defined on the manifold, a new type of differentiation, covariant differentiation, is defined as

$$\nabla_{\eta} T^{\alpha \cdots}_{\beta \ldots} = \partial_{\eta} T^{\alpha \cdots}_{\beta \ldots} + \Gamma^{\alpha}_{\mu\eta} T^{\mu \cdots}_{\beta \ldots} + \cdots - \Gamma^{\mu}_{\beta\eta} T^{\alpha \cdots}_{\mu \ldots} - \cdots \tag{25}$$

In order to guarantee that $\nabla_{\alpha} X^{\beta}$ transforms like a tensor the affine connection must transform like

$$\Gamma'^{\alpha}_{\beta\gamma} = \frac{\partial x'^{\alpha}}{\partial x^{\mu}} \frac{\partial x^{\nu}}{\partial x'^{\beta}} \frac{\partial x^{\eta}}{\partial x'^{\gamma}} \Gamma^{\mu}_{\nu\eta} - \frac{\partial x^{\mu}}{\partial x'^{\beta}} \frac{\partial x^{\nu}}{\partial x'^{\gamma}} \frac{\partial^2 x'^{\alpha}}{\partial x^{\mu} \partial x^{\nu}} \tag{26}$$

under a co-ordinate transformation. Next, define on the manifold a symmetric tensor $g_{\alpha\beta}$ called the metric. With the metric the four-dimensional line element takes the form

$$(\mathrm{d}s)^2 = g_{\alpha\beta}\, \mathrm{d}x^{\alpha}\, \mathrm{d}x^{\beta} \tag{27}$$

The metric can also be used to lower and raise indices: $X_{\alpha} = g_{\alpha\beta} X^{\beta}$. A metric is called flat if there exists a co-ordinate system in which $g_{\alpha\beta} = \mathrm{diag}(\pm 1, \ldots, \pm 1)$ everywhere. From the definition of a tensor and its covariant differentiation it is clear that if a certain tensor equation holds in a specific co-ordinate system it will also hold in a general co-ordinate system. A connection between the affine connection and the metric is now deduced. In Cartesian co-ordinates, where $g_{\alpha\beta} = \mathrm{diag}(1, 1, 1)$, $\nabla_{\beta} X_{\alpha} = g_{\alpha\lambda} \nabla_{\beta} X^{\lambda}$. This also holds in general co-ordinates. From this it can be deduced that $\nabla_{\beta} g_{\alpha\lambda} = 0$. In Cartesian co-ordinates and consequently in general co-ordinates we have $\nabla_{\alpha} \partial_{\beta} \phi = \partial_{\beta} \nabla_{\alpha} \phi$, thus $\Gamma^{\mu}_{\alpha\beta} = \Gamma^{\mu}_{\beta\alpha}$. From the symmetry of the affine connection and the fact that $\nabla_{\beta} g_{\alpha\lambda} = 0$ it follows that

$$\Gamma^{\gamma}_{\beta\mu} = \frac{1}{2} g^{\alpha\gamma} (\partial_{\mu}(g_{\alpha\beta}) + \partial_{\beta}(g_{\alpha\mu}) - \partial_{\alpha}(g_{\beta\mu})) \tag{28}$$

It is now possible to write down special relativity in tensor form. Events in space time are represented by the four vector:

$$x^{\alpha} = (ct, x, y, z) \tag{29}$$

where $\alpha = 0, 1, 2, 3$. A Lorentz transformation can be written more compactly as

$$x'^{\alpha} = L^{\alpha}_{\beta} x_{\beta}, \quad L^{\alpha}_{\beta} = \frac{\partial x'^{\alpha}}{\partial x^{\beta}} \tag{30}$$

The invariant line element is

$$(\mathrm{d}s)^2 = c^2(\mathrm{d}t)^2 - (\mathrm{d}x)^2 - (\mathrm{d}y)^2 - (\mathrm{d}z)^2 = \eta_{\alpha\beta}\,\mathrm{d}x^{\alpha}\,\mathrm{d}x^{\beta} \tag{31}$$

where $\eta_{\alpha\beta} = \mathrm{diag}(1, -1, -1, -1)$ is the Minkowski metric. The time that elapses on the clock that is moving with a particle is called the proper time. It follows from $(\mathrm{d}\tau)^2 = (\mathrm{d}s)^2/c^2$ and is defined as

$$\tau = \int_{t_0}^{t_1} \sqrt{\left(1 - \frac{\mathbf{u}\cdot\mathbf{u}}{c^2}\right)}\,\mathrm{d}t \tag{32}$$

where $\mathbf{u} = \mathrm{d}\mathbf{x}/\mathrm{d}t$ is the particle speed. Now we can define the four-velocity vector:

$$U^{\alpha} = \frac{\mathrm{d}x^{\alpha}}{\mathrm{d}\tau} = \left(\Gamma c, \Gamma \frac{\mathrm{d}\mathbf{x}}{\mathrm{d}t}\right) \tag{33}$$

And finally the four-momentum is defined as

$$P^{\alpha} = m_{\mathrm{r}} U^{\alpha} = \left(E/c, m_{\mathrm{r}}\Gamma \frac{\mathrm{d}\mathbf{x}}{\mathrm{d}t}\right) \tag{34}$$

This enables us to describe the interaction of particles in a Lorentz-invariant way.

2. SPECIAL RELATIVISTIC HYDRODYNAMICS

In this section, the equations describing a relativisticly flowing fluid are derived, following the book of Schutz [6].

2.1. Particle-conservation equation

First, consider conservation of particles. The number of particles in a control volume moving with the fluid is the same for an observer moving with the control volume (rest frame) as for an observer standing still and watching the moving control volume (laboratory frame). What differs is the number density (n), i.e. the number of particles (N) per unit volume (V), in both frames. Assume the x-axis of the laboratory frame is oriented parallel to the direction of movement of the control volume. Furthermore, it is assumed that the particles in the infinitesimally small control volume all move with the same fluid speed $\mathbf{u}$[¶] with respect to the laboratory frame. To connect the number density in both frames the length contraction formula (10) is used:

$$n = \frac{N}{V} = \frac{N}{\Delta x \Delta y \Delta z} = \frac{N}{\sqrt{(1 - \mathbf{u}\cdot\mathbf{u}/c^2)}\,\Delta x' \Delta y' \Delta z'} = \Gamma \frac{N}{V_{\mathrm{r}}} = \Gamma n_{\mathrm{r}} \tag{35}$$

[¶]The components of $\mathbf{u}$ are u^i with $i = 1, 2, 3$.

Another important quantity is the particle flux. It is defined as nu^i, the number of particles crossing a surface perpendicular to the flow direction per unit of time and per unit of area. If one considers a cube with volume l^3 placed in the origin of a co-ordinate system, then conservation of particles means that the change of particles per unit of time in the cube must equal the net flux of particles into the cube:

$$\begin{aligned}\frac{\partial}{\partial t}(l^3 n) = l^2\,((nu^i)_{x=0} - (nu^i)_{x=l} + \\ (nu^j)_{y=0} - (nu^j)_{y=l} + \\ (nu^k)_{z=0} - (nu^k)_{z=l})\end{aligned} \tag{36}$$

Taking the limit $l \to 0$ in the above equation results in $\partial(n_r U^\alpha)/\partial x^\alpha = 0$, or in a general co-ordinate system

$$\nabla_\alpha (n_r U^\alpha) = 0 \tag{37}$$

2.2. *Energy-momentum equations*

Next the energy-momentum tensor will be dealt with. Again a control volume V containing a fluid with mass M and energy E is considered. The density of a quantity is defined as this quantity per unit of volume and the flux of a quantity is defined as this quantity passing a surface perpendicular to the flow direction per unit of time per unit of area. In general the energy momentum tensor $T^{\alpha\beta}$ is defined as

- T^{00}: Energy density ($E/V = e$).
- T^{0i}: Energy flux across surface A^i ($= eu^i$).
- T^{i0}: Momentum density in i-direction ($Mu^i/V = \rho u^i$).
- T^{ij}: Momentum flux in i-direction across surface A^j.

Assume we are in the local rest frame of the fluid. Then along the surface A^j a fluid element exerts a force F^i in the i-direction. By Newton's law $\mathrm{d}p^i/\mathrm{d}t = F^i$, which is now valid because we are in the local rest frame, we have momentum flux in the i-direction across the surface A^j and so $T^{ij} = \text{momentum}/(\text{time} \times \text{area}) = F^i/A^j$. If there is no viscosity then there are no forces parallel to the surface of the control volume, $T^{ij} = 0$ if $i \neq j$. The tensor $T^{\alpha\beta}$ has the property $(1/c)T^{0i} = cT^{i0}$ because $eu^i/c = c\rho u^i$, and the property $T^{ij} = T^{ji}$ because there is no net torque allowed on a fluid element in rest. Assuming conservation of momentum and energy, the energy-momentum equations can be deduced in the same way as the particle conservation equation was derived:

$$\nabla_\alpha T^{\alpha\beta} = 0 \tag{38}$$

An ideal fluid is assumed, meaning that there is no viscosity and that there is no heat conduction. In the local rest frame the fluid is not moving and the only force exerted by a fluid element is a pressure force. For the momentum flux in the i-direction perpendicular to the surface A^i it is found that $T^{ii} = F^i/A^i = p$, with p the pressure. The energy density is $T^{00} = e$.

The energy-momentum tensor for the fluid at rest is then

$$T^{\alpha\beta} = \begin{pmatrix} e & 0 & 0 & 0 \\ 0 & p & 0 & 0 \\ 0 & 0 & p & 0 \\ 0 & 0 & 0 & p \end{pmatrix} \tag{39}$$

where $e = n_r m_r c^2 + \varepsilon' = \rho_r c^2 + \varepsilon'$ is the energy density and ε' is the internal energy density. In general the energy-momentum tensor is written as

$$T^{\alpha\beta} = (e + p)U^\alpha U^\beta / c^2 + p\eta^{\alpha\beta} \tag{40}$$

Equation (40) is an extension of Equation (39) to a general frame. This is the most simple form one can think of which reduces to (39) if $U^\alpha = (c, 0, 0, 0)$ and reduces to the Euler equations if $u/c \to 0$, as is shown in the following.

2.3. *Asymptotic equations for low Lorentz-factor limits*

In order to take the limit $u/c \to 0$ the Lorentz factor is expanded in terms of u/c: $\Gamma = 1 + \frac{1}{2}u^2/c^2 + O(u^4/c^4)$ and $\Gamma^2 = 1 + u^2/c^2 + O(u^4/c^4)$. We start with the particle conservation equation

$$\frac{1}{c}\frac{\partial(cn_r m_r \Gamma)}{\partial t} + \frac{\partial(n_r m_r \Gamma u^i)}{\partial x^i} = 0 \tag{41}$$

The original particle conservation equation has been multiplied by m_r, the rest mass of a fluid particle which is a constant. Expansion of the Lorentz factor in (41) leads to

$$\frac{\partial \rho_r}{\partial t} + \frac{\partial(\rho_r u^i)}{\partial x^i} = -\frac{1}{2}\frac{\partial}{\partial t}\left(\rho_r\left(\frac{u}{c}\right)^2\right) - \frac{1}{2}\frac{\partial}{\partial x^i}\left(\rho_r u^i\left(\frac{u}{c}\right)^2\right) + O\left(\frac{u^4}{c^4}\right) \tag{42}$$

Next, consider the energy equation

$$\frac{1}{c}\frac{\partial(\Gamma^2(e + p) - p)}{\partial t} + \frac{\partial(\Gamma^2(e + p)u^i/c)}{\partial x^i} = 0 \tag{43}$$

After substitution of the expanded Lorentz factor the energy equation transforms into

$$\begin{aligned} c^2\left(\frac{\partial \rho_r}{\partial t} + \frac{\partial(\rho_r u^i)}{\partial x^i}\right) + \frac{\partial}{\partial t}(\rho_r u^2 + \varepsilon') + \frac{\partial}{\partial x^i}(u^i(\rho_r u^2 + \varepsilon' + p)) \\ + \frac{\partial}{\partial t}\left((\varepsilon' + p)\left(\frac{u^2}{c^2}\right)\right) + \frac{\partial}{\partial x^i}\left((\varepsilon' + p)\left(\frac{u^2}{c^2}\right)u^i\right) + O\left(\frac{u^4}{c^4}\right) = 0 \end{aligned} \tag{44}$$

After substitution of the expanded particle conservation equation (42) the energy equation can be written in the form

$$\frac{\partial}{\partial t}\left(\frac{1}{2}\rho_r u^2 + \varepsilon'\right) + \frac{\partial}{\partial x^i}\left(u^i\left(\frac{1}{2}\rho_r u^2 + \varepsilon' + p\right)\right) = O\left(\frac{u^4}{c^2}\right) \tag{45}$$

The expansion of the momentum equation

$$\frac{1}{c}\frac{\partial}{\partial t}\left(\frac{e+p}{c^2}\Gamma^2 u^i c\right)+\frac{\partial}{\partial x^j}\left(\frac{e+p}{c^2}\Gamma^2 u^i u^j + p\delta^{ij}\right)=0 \tag{46}$$

is straightforward and results in

$$\frac{\partial}{\partial t}(\rho_{\mathrm{r}} u^i)+\frac{\partial}{\partial x^j}(\rho_{\mathrm{r}} u^i u^j + p\delta^{ij})=O\left(\frac{u^2}{c^2}\right) \tag{47}$$

In the limit $u/c\to 0$ the right-hand sides of Equations (42), (45) and (47) vanish and the Euler equations are recovered. In the following the speed of light is put to unity ($c=1$). This corresponds to the scaling

$$\begin{pmatrix} u^i \\ p \\ \varepsilon' \\ t \end{pmatrix} \to \begin{pmatrix} u^i c \\ pc^2 \\ \varepsilon' c^2 \\ t/c \end{pmatrix} \tag{48}$$

3. RIEMANN PROBLEM IN SRHD

The SRHD equations are hyperbolic for causal equations of state [7].[‖] In order to test a numerical method a solution to the Riemann problem is necessary. This solution was found by Martí [8]. The 1D SRHD equations follow from Equations (37), (38) and (40). The following steps are performed: (i) the particle conservation equation is multiplied by a constant m_{r}, (ii) the internal energy is redefined as $\varepsilon'=\rho_{\mathrm{r}}\varepsilon$ with $\varepsilon=$(internal energy)/(unit of mass), (iii) the enthalpy is introduced as $h=1+\varepsilon+p/\rho_{\mathrm{r}}$ and (iv) in order to avoid accuracy problems when numerically solving the SRHD equations the particle conservation equation is subtracted from the energy equation. The subscript r in ρ_{r} is dropped from now on. In conservative form the 1D SRHD equations are

$$\frac{\partial \mathbf{U}}{\partial t}+\frac{\partial \mathbf{F}}{\partial x}=0 \tag{49}$$

with the conserved variables:

$$\mathbf{U}=\begin{pmatrix} D \\ S \\ \tau \end{pmatrix}=\begin{pmatrix} \rho\Gamma \\ \rho h\Gamma^2 v \\ \rho h\Gamma^2 - p - \rho\Gamma \end{pmatrix} \tag{50}$$

[‖]Meaning that the speed of sound is less than the speed of light.

and the fluxes:

$$\mathbf{F} = \begin{pmatrix} Dv \\ Sv + p \\ S - Dv \end{pmatrix} \tag{51}$$

The system is balanced with an equation of state, usually the ideal gas law is used:

$$\varepsilon = \frac{p}{\rho(\gamma - 1)} \tag{52}$$

with γ the ratio of specific heats. To transform from conserved variables to primitive variables (ρ, v, p) is not straightforward and a non-linear equation must be solved numerically.

In the following the spectral decomposition of the 1D SRHD equations is calculated. If we take $p = p(\rho, \varepsilon)$ and $\mathbf{F} = \mathbf{F}(\mathbf{w}(\mathbf{U}))$ then the system of equations (49) can be written as

$$\frac{\partial \mathbf{U}}{\partial t} + \frac{\partial \mathbf{F}}{\partial \mathbf{w}} \left(\frac{\partial \mathbf{U}}{\partial \mathbf{w}} \right)^{-1} \frac{\partial \mathbf{U}}{\partial x} = 0 \tag{53}$$

with the primitive variables

$$\mathbf{w} = \begin{pmatrix} \rho \\ v \\ \varepsilon \end{pmatrix} \tag{54}$$

After a lengthy calculation it follows that the eigenvalues and eigenvectors of $(\partial \mathbf{F}/\partial \mathbf{w})(\partial \mathbf{U}/\partial \mathbf{w})^{-1}$ are given by

$$\begin{aligned} \lambda_0 &= v \\ \lambda_\pm &= \frac{v \pm c_s}{1 \pm v c_s} \\ \mathbf{r}_0 &= \left(\frac{\kappa}{h\Gamma(\kappa - c_s^2 \rho)}, v, 1 - \frac{\kappa}{h\Gamma(\kappa - c_s^2 \rho)} \right)^{\mathrm{T}} \\ \mathbf{r}_\pm &= \left(1, h\Gamma\lambda_\pm \left(\frac{1 - v^2}{1 - v\lambda_\pm} \right), h\Gamma \left(\frac{1 - v^2}{1 - v\lambda_\pm} \right) - 1 \right)^{\mathrm{T}} \end{aligned} \tag{55}$$

with $\kappa = \partial p/\partial \varepsilon$ and c_s the speed of sound.

To the system of equations (49) initial conditions are added:

$$(p, \rho, v)(x, 0) = \begin{cases} (p_L, \rho_L, v_L) & \text{if } x < 0 \\ (p_R, \rho_R, v_R) & \text{if } x > 0 \end{cases} \tag{56}$$

The SRHD equations together with the above initial conditions constitute the special relativistic Riemann problem. As in the classical Riemann problem it contains three types of waves: shock, rarefaction and contact discontinuity waves. The solution is schematically represented

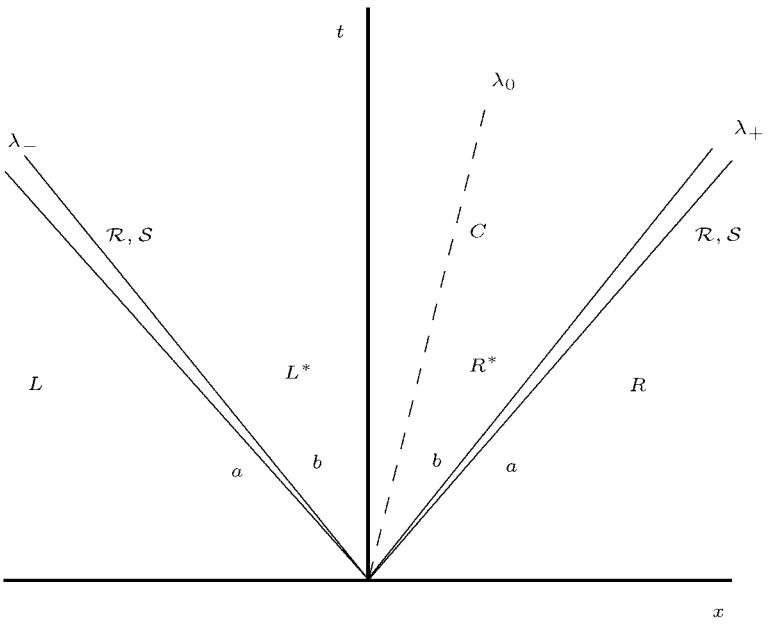

Figure 1. Characteristics in the SRHD Riemann problem. $\mathscr{R}, \mathscr{S}$ stands for rarefaction or shock wave, respectively, and C for contact discontinuity.

in Figure 1. The L, L^*, R^*, R represent constant state solutions, the dashed line is a contact discontinuity and the double lines represent a shock- or a rarefaction wave. The states L and R are known. Also, plotted in the figure are the labels a, b to indicate a state (a)head or (b)ehind a shock/rarefaction. Across the contact discontinuity $p_{L^*} = p_{R^*}$ and $v_{L^*} = v_{R^*}$; only the density makes a jump across the contact discontinuity. A rarefaction is formed if $p_b \leqslant p_a$, else a shock is formed.

3.1. *Rarefaction waves*

For $t > 0$ self-similar solutions of the Riemann problem can be found. They depend on the variable $\xi = x/t$. Just as in classical gas dynamics it can be deduced that the entropy density, s, is constant along fluid particle paths

$$U^\alpha \frac{\partial s}{\partial x^\mu} = 0 \tag{57}$$

And after substitution of the similarity variable the above equation transforms to

$$(v - \xi)\frac{\mathrm{d}s}{\mathrm{d}\xi} = 0 \tag{58}$$

Therefore, self-similar flow is isentropic and

$$\frac{p}{\rho^\gamma} = \text{constant} \tag{59}$$

In general the speed of sound is defined as

$$hc_s^2 = \frac{\partial p}{\partial \rho} + \frac{p}{\rho^2}\frac{\partial p}{\partial \varepsilon} (= \gamma \frac{p}{\rho}, \text{ ideal gas}) \tag{60}$$

If the flow is isentropic, then:**

$$c_s^2 = \frac{1}{h}\left(\frac{\partial p}{\partial \rho}\right)_s \tag{61}$$

Together with $p_x = \gamma p \rho_x/\rho$ and $c_s^2 = \gamma p/(\rho h)$ the particle conservation equation and the momentum equation can be transformed to

$$\begin{pmatrix} (v-\xi) & \rho\Gamma^2(1-\xi v) \\ (1-\xi v)c_s^2 & (v-\xi)\rho\Gamma^2 \end{pmatrix} \begin{pmatrix} \rho_\xi \\ v_\xi \end{pmatrix} = 0 \tag{62}$$

If the determinant is zero the system has a solution. This is the case if

$$\xi = \frac{v \mp c_s}{1 \mp c_s v} \tag{63}$$

and

$$\frac{c_s \, \mathrm{d}\rho}{\rho} \pm \Gamma^2 \, \mathrm{d}v = 0 \tag{64}$$

where $-(+)$ represents a wave to the left(right). From Equation (64) the Riemann invariants can be calculated:

$$\frac{1+v}{1-v}\left(\frac{\sqrt{\gamma-1}+c_s}{\sqrt{\gamma-1}-c_s}\right)^{\pm 2/\sqrt{(\gamma-1)}} = \text{constant} \tag{65}$$

The above equation can be used to express v_b in terms of quantities ahead of the wave and p_b:

$$v_b = \frac{(1+v_a)A_\pm(p_b) - (1-v_a)}{(1+v_a)A_\pm(p_b) + (1-v_a)} \tag{66}$$

$$A_\pm(p_b) = \left(\frac{(\sqrt{\gamma-1} - c_s(p_b))(\sqrt{\gamma-1} + c_s(p_a))}{(\sqrt{\gamma-1} + c_s(p_b))(\sqrt{\gamma-1} - c_s(p_a))}\right)^{\pm 2/\sqrt{(\gamma-1)}} \tag{67}$$

The velocity field inside the rarefaction wave as a function of ξ can be solved from Equations (63) and (66). Thermodynamic quantities inside the rarefaction directly follow from Equations (59) and (61).

**For a hot gas in the relativistic case, $(p/\rho \sim T \to \infty)$ it is found that $c_s = \sqrt{\gamma-1}$. And in the non-relativistic case $c_s^2 = \gamma p/\rho \sim \gamma T$.

3.2. Shock waves

Shocks are also solutions to the SRHD Riemann problem. The shock front is described by a Lorentz-invariant surface $\Sigma(x,t)=0$,

$$\Sigma=\Gamma_s(x-v_s t) \tag{68}$$

where v_s is the shock speed and Γ_s the corresponding Lorentz factor. The normal vector to this surface is: $n^\mu=\Gamma_s(-v_s,1,0,0)$. After the use of four-dimensional version of the Gauss law the shock relations are

$$[\rho U^\mu]n_\mu=0 \tag{69}$$

and

$$[T^{\mu\nu}]n_\mu=0 \tag{70}$$

where $[f]=f_a-f_b$. From the continuity condition (69) it follows that

$$\Gamma_s D_a(v_s-v_a)=\Gamma_s D_b(v_s-v_b) \tag{71}$$

and the invariant mass flux is defined as

$$j=\Gamma_s D_a(v_s-v_a) \tag{72}$$

The relativistic Rankine Hugoniot conditions can be written as

$$[v]=\frac{-j}{\Gamma_s}\left[\frac{1}{D}\right] \tag{73}$$

$$[p]=\frac{j}{\Gamma_s}\left[\frac{S}{D}\right] \tag{74}$$

$$[vp]=\frac{j}{\Gamma_s}\left[\frac{\tau}{D}\right] \tag{75}$$

These conditions can be used to calculate the flow speed behind the shock, v_b,

$$v_b=\frac{h_a\Gamma_a v_a+\Gamma_s(p_b-p_a)/j}{h_a\Gamma_a+(p_b-p_a)(\Gamma_s v_a/j+1/(\rho_a\Gamma_a))} \tag{76}$$

After calculating $[T^{\mu\nu}]n_\mu n_\nu=0$ an expression for j can be found:

$$j^2=\frac{-[p]}{[h/\rho]} \tag{77}$$

With the use of the Taub adiabat an expression for h_b can be found. The Taub adiabat results from adding $[T^{\mu\nu}]n_\nu(hU_\mu)_a$ and $[T^{\mu\nu}]n_\nu(hU_\mu)_b$;

$$\left(1+(\gamma-1)\frac{p_a-p_b}{\gamma p_b}\right)h_b^2-(\gamma-1)\frac{p_a-p_b}{\gamma p_b}h_b+\frac{p_a-p_b}{\rho_a}h_a-h_a^2=0 \tag{78}$$

Solving this equation and disregarding the negative solution gives an expression for $h_b(p_b)$. Only an expression for v_s is needed. It results from the definition of the mass flow j:

$$v_s^{\pm} = \frac{\rho_a^2 \Gamma_a^2 v_a \pm j^2 \sqrt{1 + (\rho_a/j)^2}}{\rho_a^2 \Gamma_a^2 + j^2} \tag{79}$$

If $j<0$ then take v_s^- and if $j>0$ then take v_s^+. All the ingredients are now present to solve the relativistic Riemann problem.

3.3. Solution

The states L and R, see Figure 1, can be connected from the left to the right by a shock/rarefaction wave followed by a contact discontinuity and finally again a shock/rarefaction wave. The λ_- wave is described by (66), if $p^* \leqslant p_L$, or (76), if $p^* > p_L$, with $a = L$, $b = L^*$ and by symmetry similar expressions for the λ_+ wave. Next, the two expressions for the velocities are set equal and are solved for p^*. In practice an iterative procedure is needed because p^* is not known in advance. If p^* is found then automatically v^* is known. In the case of a shock the density ρ_{I^*} ($I^* = L^*, R^*$) follows from (combining the expressions for the enthalpy and for the internal energy density):

$$\rho_{I^*} = \frac{\gamma p_{I^*}}{(\gamma - 1)(h_{I^*} - 1)} \tag{80}$$

and from expression (78) for h_{I^*}. The mass flow across the shock and the shock speed follow from Equations (77) and (79), respectively. In the case of a rarefaction wave ρ_{I^*} follows from the isentropic equation of state (59). The velocities of the head and the tail of the rarefaction wave are found from Equation (63) with the appropriate limiting values substituted.

4. NUMERICAL SOLUTION

The method described in Section 3 can be used in the Godunov scheme [9]. A Fortran program to calculate the exact one-dimensional SRHD Riemann problem can be found on the world wide web [10]. It can be used to calculate the fluxes needed in the Godunov scheme. A mesh is defined in the (x,t)-plane in order to discretize Equation (49). The points on the mesh are at locations $(x_i = ih_x, t^n = nh_t)$ with $i = 0, \ldots, M$ and $n = 0, \ldots, N$. The discrete values of $\boldsymbol{U}(x,t)$ at (ih_x, nh_t) will be denoted by $\boldsymbol{U}_i^n$. The conserved variables $\boldsymbol{U}(x,t)$ are advanced in time in the following way:

$$\boldsymbol{U}_i^{n+1} = \boldsymbol{U}_i^n + \frac{h_t}{h_x}(\boldsymbol{F}_{i-1/2} - \boldsymbol{F}_{i+1/2}) \tag{81}$$

where $\boldsymbol{F}_{i+1/2} = \boldsymbol{F}(\boldsymbol{U}_{i+1/2}(0))$ with $\boldsymbol{U}_{i+1/2}(0)$ the similarity solution at $x/t = 0$ of the Riemann problem at the cell boundary $i + \frac{1}{2}$ with left and right initial data $\boldsymbol{U}_i^n$ and $\boldsymbol{U}_{i+1}^n$, respectively. To ensure that no waves interact within a cell, the time step must satisfy the condition:

$$h_t = \sigma \frac{h_x}{S_{\max}^n}, \quad 0 < \sigma \leqslant 1 \tag{82}$$

where σ is the Courant number and $S_{\max}^n$ the largest signal velocity in the domain at a certain time step t^n.

Table I. Left and right initial values for problem 1, 2.

	Problem 1		Problem 2	
	L	R	L	R
p	13.3	0.01	1000.0	0.01
ρ	10.0	1.0	1.0	1.0
v	0.0	0.0	0.0	0.0

Two model problems have been considered on a domain $x \in [0,1]$ with for the number of grid points $M = 400$ and for the ratio of specific heats $\gamma = \frac{5}{3}$. The initial left state for $x \leqslant 0.5$ and the initial right state for $x > 0.5$ are given in Table I. Transmissive boundary conditions have been used.

In Figures 2 and 3 the exact solution and the numerical solution for Problem 1 and 2 in the non-relativistic and in the relativistic case are depicted. Note that in Problem 2, the higher Lorentz-factor case, the shock wave is pushed out of phase by the diffusing contact discontinuity. Important differences between the relativistic solution and the non-relativistic one are:

- The relativistic rarefaction solution of the flow velocity is non-linear.
- The relativistic velocities are limited by the speed of light.
- The density jump is a function of the pressure jump. From the Taub adiabat (78) and the ideal gas law (52) it follows that for $p_b/p_a \to \infty$ the density jump approaches:

$$\frac{\rho_b}{\rho_a} = \sqrt{\frac{\gamma p_a/\rho_a}{(\gamma-1)(\gamma-1+\gamma p_a/\rho_a)}}\sqrt{\frac{p_b}{p_a}} \tag{83}$$

  In the non-relativistic case, after the introduction of dimensional quantities in the Taub adiabat, the terms with p_a/ρ_a drop because $p_a/\rho_a \to p_a/(c^2\rho_a) \to 0$ and the density jump approaches:

$$\frac{\rho_b}{\rho_a} = \frac{\gamma+1}{\gamma-1} \tag{84}$$

  In the relativistic case $\rho_b/\rho_a \to \infty$ for $p_b/p_a \to \infty$.
- The relativistic density shell (in between contact discontinuity and shock wave) can be extremely narrow as a result of the Lorentz contraction.

In Figure 4, a detail of the density profile is shown for different numbers of grid points. It shows the slow convergence to the exact solution of a first-order (in time and in space) method. Better results can be obtained by higher-order methods like PHM [11], PPM [12] or by grid refinement techniques.

In the following section, an example is given of how the introduction of an extra velocity component aggravates the convergence of the numerical solution to the exact solution.

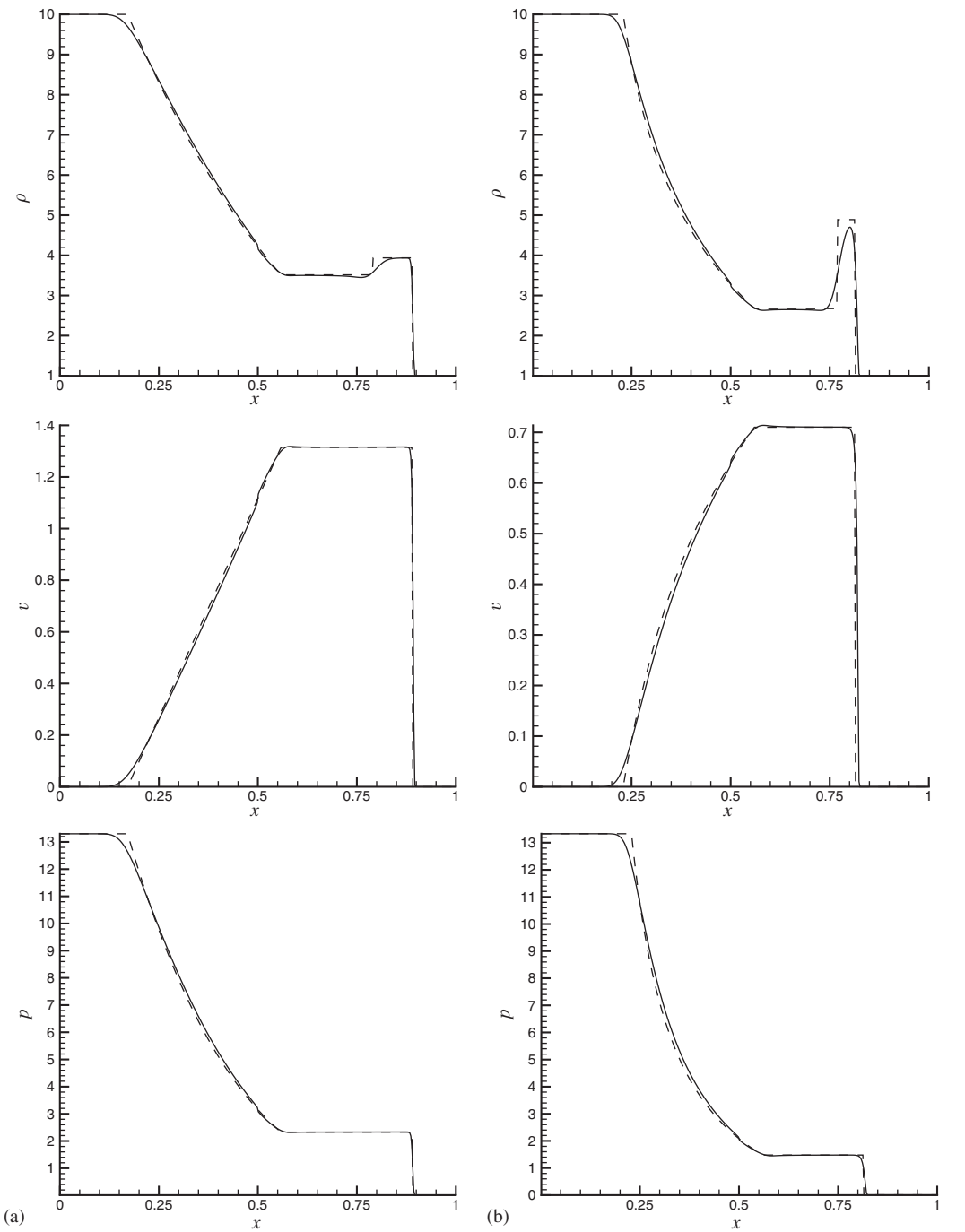

Figure 2. Problem 1 ($M = 400, \gamma = 5/3$): first-order accurate (solid, $\sigma = 0.7$) and exact discrete (dashed): (a) Non-relativistic, $t = 0.221$. (b) Relativistic, $t = 0.378$.

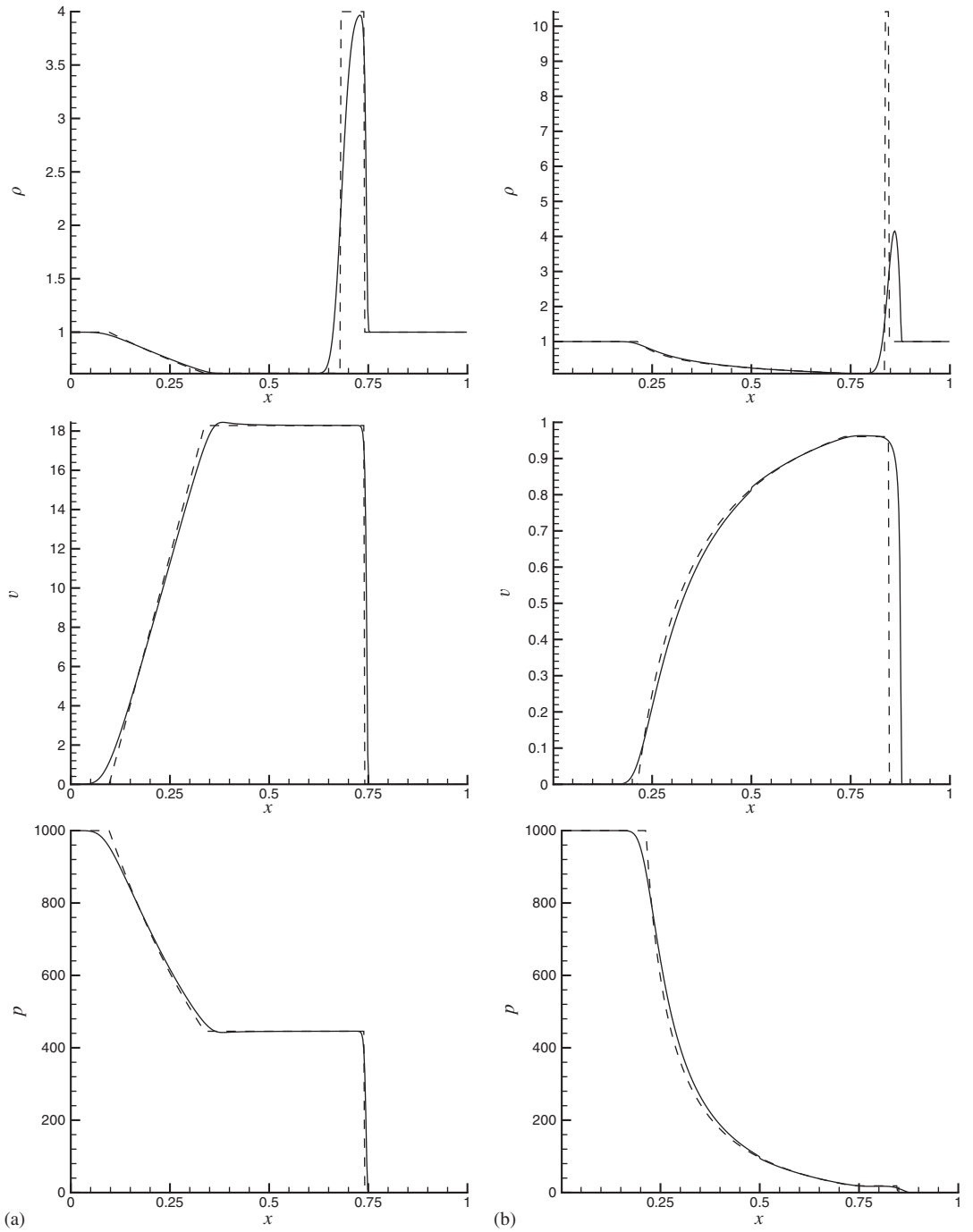

Figure 3. Problem 2 ($M = 400, \gamma = 5/3$): first-order accurate (solid, $\sigma = 0.7$) and exact discrete (dashed): (a) Non-relativistic, $t = 001$. (b) Relativistic, $t = 0.351$.

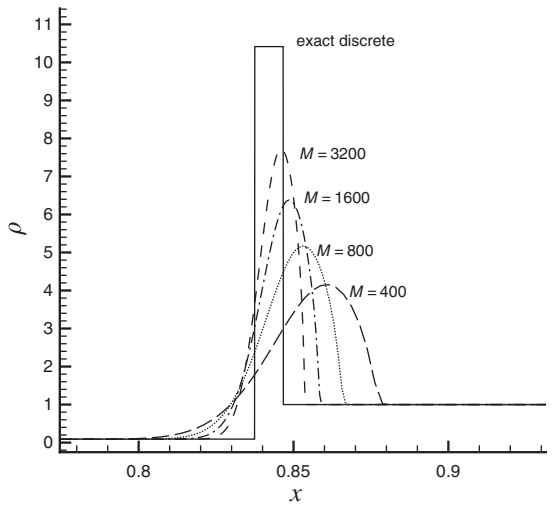

Figure 4. Detail of density distributions for Problem 2, $t = 0.351$, $\sigma = 0.7$, $\gamma = 5/3$.

4.1. Quasi-1D SRHD

In order to construct a scheme that can handle more than one space dimension the Riemann solver has to take care of the tangential velocity. This is not as easy as in the Euler case because all equations are connected to each other through the Lorentz factor and the enthalpy. In contrast to the Euler case the tangential velocity makes a jump at the shock location. In the quasi-1D case the conserved variables and fluxes in Equation (49) are

$$\mathbf{U} = \begin{pmatrix} D \\ S^x \\ S^y \\ \tau \end{pmatrix} = \begin{pmatrix} \rho\Gamma \\ \rho h \Gamma^2 v^x \\ \rho h \Gamma^2 v^y \\ \rho h \Gamma^2 - p - \rho\Gamma \end{pmatrix}, \quad \mathbf{F} = \begin{pmatrix} Dv^x \\ S^x v^x + p \\ S^y v^x \\ (\tau + p) v^x \end{pmatrix} \tag{85}$$

where $\Gamma = 1/\sqrt{1 - v_x^2 - v_y^2}$. The shock relations given in Equations (69), (70) can be put in the form

$$\begin{aligned} [v^x] &= -\frac{j}{\Gamma_s}\left[\frac{1}{D}\right][h\Gamma v^y] = 0 \\ [p] &= \frac{j}{\Gamma_s}\left[\frac{S^z}{D}\right][v^x p] = \frac{j}{\Gamma_s}\left[\frac{\tau}{D}\right] \end{aligned} \tag{86}$$

At the contact discontinuity ($j = 0$) we have that the pressure and the normal velocity are continuous and that the density and the tangential velocity are discontinuous. The eigenvalues

Table II. Left and right initial values for Problem 3.

	Problem 3	
	L	R
p	1.0	1.0
ρ	1.0	1.0
v_x	0.4	0.0
v_y	0.9	0.0

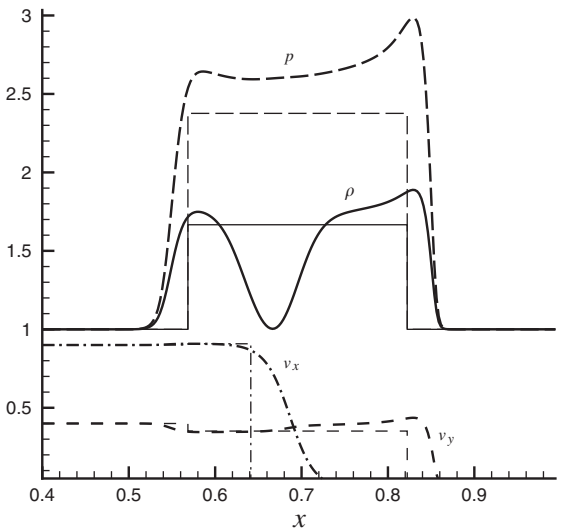

Figure 5. Numerical (thick lines) and exact (thin lines) solutions of Problem 3, $t = 0.402$, $\sigma = 0.7$, $\gamma = 5/3$.

of the Jacobian $\partial\mathbf{F}/\partial\mathbf{U}$ are

$$\lambda_0 = v^x, \quad \lambda_\pm = \frac{v^x(1-c_s^2) \pm c_s\sqrt{(1-\mathbf{v}\cdot\mathbf{v})(1-\mathbf{v}\cdot\mathbf{v}c_s^2 - v_x^2(1-c_s^2))}}{1-\mathbf{v}\cdot\mathbf{v}c_s^2} \tag{87}$$

They are used to calculate the fluxes at the cell interfaces according to the Lax–Friedrichs flux:

$$\boldsymbol{F}_{i+1/2} = \frac{1}{2}(\boldsymbol{F}_i^n + \boldsymbol{F}_{i+1}^n - C_{i+\frac{1}{2}}^{\max}(\boldsymbol{U}_{i+1}^n - \boldsymbol{U}_i^n)) \tag{88}$$

where

$$C_{i+\frac{1}{2}}^{\max} = \max[C_i^{\max}, C_{i+1}^{\max}], \quad C_i^{\max} = (\max_p[|\lambda_p|])_i \tag{89}$$

In Table II, Problem 3 is defined and the results are plotted in Figure 5. An exact Riemann solver for the quasi 1D situation can be constructed in the same way as for the pure 1D

case, see Reference [13]. Figure 5 shows that there is a large discrepancy between the numerical solution and the exact solution near the CD. The most striking error is the dip in the density where it should be constant. Numerical calculations show that this dip only narrows for decreasing mesh size. Further numerical analyzis and possible remedies are given in a forthcoming article.

5. OVERVIEW NUMERICAL METHODS

In the following a short description is given of the numerical methods used so far in SRHD. Only the high resolution shock capturing (HRSC) methods are mentioned because they seem to be the most effective [10, p. 54] for solving the SRHD equations in the case of astrophysical problems. A good description of the different methods can be found in Reference [14]:

- Godunov method: Martí and Müller [15] have used an exact Riemann solver in combination with the piecewise parabolic method (PPM) of Collela and Woodward [12] to solve the 1D SRHD equations. The PPM method is used for the reconstruction of the primitive variables at cell faces. The scheme is second-order accurate in time and space. In Reference [13] they developed an exact Riemann solver for the general multi-dimensional SRHD equations. They found that in contrast to the Euler equations the tangential (to the shock surface) velocity components are not constant over a shock or rarefaction wave in the laboratory frame.
- Glimm's method: Wen [16] has used Glimm's random choice method [17] to numerically solve the 1D SRHD equations. This method uses an exact Riemann solver but in contrast to the Godunov method where an average of the solution of the local Riemann problem is used to advance in time, now a randomly chosen point in the solution of the local Riemann problem is used. The method is only useful in one dimension. It produces shocks and contact discontinuities which are completely free of diffusion and dispersion errors.
- Two shock approximation [18]: It assumes that the local Riemann problem is built up of two shocks. Consequently there are problems to be expected with strong rarefaction waves. If it is used in two dimensions it has the advantage that no extra differential equation has to be solved for the coupling between normal and tangential velocity component in the case of a rarefaction wave. The shock conditions for the tangential velocity components are still to be solved. Balsara [19] circumvents these conditions and transforms to the shock frame where the tangential velocity components are continuous across a shock. Dai and Woodward [20] directly use the shock conditions for the tangential velocity components.
- Roe-type solver: In the work of Eulderink *et al.* [21, 22] a local linearization of a Roe-type approximate Riemann solver [23] is applied in combination with Roe-average state variables to calculate the Jacobian at cell faces. They demonstrate that for a 1D test problem calculations of Lorentz factors up to 625 are possible. Instead of taking the Roe-averages to calculate the Jacobian at cell interfaces the arithmetic average of the primitive variables can be used, this has been done by Romero *et al.* [24] in a 1D general relativistic hydrodynamics code. In the local characteristic approach [25] a local linearization of the system of equations has been performed by defining a set of characteristic variables, which obey a system of uncoupled scalar equations. This approach is used by Marquina

et al. [11] and Dolezal and Wong [26] in combination with a higher-order characteristic flux reconstruction method, namely PHM [11] and ENO [26], respectively.

- Falle and Komissarov [27] apply a local linearization to the SRHD equations in primitive variable form to solve the Riemann problem. This solution is used to calculate the fluxes in the time evaluation step, which is performed in the conserved variable formulation.
- Relativistic HLL (Harten, Lax, van Leer [28]) method: Schneider *et al.* [29] use the HLL method to numerically solve the SRHD equations in 1D. In this method, the Riemann problem is reduced to a problem with a single intermediate state. The intermediate state is found by requiring consistency of the approximate Riemann solution with the integral form of the conservation laws in a grid zone. Then only lower and upper bounds for the smallest and largest signal velocities are needed. The scheme is very dissipative at contact discontinuities. The HLL method has been extended to 2D by Duncan and Hughes [30].
- Marquina's method: If no special measures are taken (addition of artificial dissipation) most Godunov-type schemes have some kind of pathology [31], for example entropy violating expansion shocks in Roe's method. Donat and Marquina [32] upgrade a scalar method proposed by Shu and Osher [33] to systems. In the scalar case Marquina's flux formula is a combination of Roe's flux and a local Lax–Friedrichs flux. For systems it is not always possible to find Roe-average values. Therefore, Marquina makes use of the left/right-eigenvectors and eigenvalues to compute the flux at the cell interfaces. The choice between Roe's solver and the Lax–Friedrichs scheme is performed in each local characteristic field. Excellent results have been obtained with this flux formula in the case of 1D and 2D ultra-relativistic flows, see Marti *et al.* [34, 35]. A 3D relativistic hydrodynamics code, GENESIS, has been developed by Aloy *et al.* [36] based on Marquina's flux.
- Symmetric TVD schemes: In the algorithm of Davis [37] a standard finite difference scheme is used and a non-linear dissipation term is added. It can be seen as a Lax–Wendroff scheme with a conservative dissipation term. In this method, there are no problem-dependent parameters and no characteristic information is needed. It has been used by Koide *et al.* [38, 39] to calculate multi-dimensional special(general) relativistic(magneto)hydrodynamic problems. So far, all these calculations were performed for low Lorentz factors.

6. CONCLUSIONS

As compared to the Euler equations, the SRHD equations are more strongly coupled because of the Lorentz factor and the enthalpy.

The structure of the relativistic Riemann problem solution is the same as in the non-relativistic case. Characteristics of the relativistic solution are: that the velocity profile is non-linear, that the velocities are limited to the speed of light and that the density jump across a shock approaches infinity if the pressure jump approaches infinity.

The Godunov scheme has been applied to solve two test problems: a mildly relativistic and an ultra-relativistic problem. The ultra-relativistic problem especially shows that the thin density shell is hard to capture with a first-order method. The smeared contact discontinuity has a negative influence on the location of the shock front.

To demonstrate the non-convergent behaviour of the approximate Riemann solver in the case of Problem 3 we used the Lax–Friedrichs flux in the Godunov scheme. It is shown that at the contact discontinuity the density is not constant as opposed to what is predicted with the exact Riemann solver.

Most known numerical methods to solve hyperbolic conservation laws are being used in SRHD. An exception is the Osher scheme [40] which is not (yet) in use. Probably, because in the Osher scheme Riemann invariants are needed and in 2D there are no analytical expressions available for these. The Roe solver captures all waves properly when equipped with an entropy fix. However, Roe-average states may be hard to find when the solver is extended to handle special relativistic magneto-hydrodynamics (SRMHD). This extension to SRMHD may also be a problem for the exact Riemann solver. To my knowledge no exact solution is available for the 1D SRMHD problem. Furthermore, the use of an exact Riemann solver may be rather time consuming. Marquina's method also captures all waves adequately and has the advantage that only the eigenvectors and eigenvalues of the considered problem are needed. A disadvantage is that it smears a steady shock as time advances.

REFERENCES

1. Aloy MA, Ibáñez JM, Martí JM, Gómez JL, Müller E. High-resolution three-dimensional simulations of relativistic jets. *Astrophysical Journal* 1999; **523**:L125–L128.
2. Piran T, Shemi A, Narayan R. Hydrodynamics of relativistic fireballs. *Monthly Notices of the Royal Astronomical Society* 1993; **263**:861–867.
3. Csernai LP. *Introduction to Relativistic Heavy Ion Collisions*. Wiley: Chichester, New York, 1994.
4. van Odyck DEA. Error reduction at the contact discontinuity in numerical special relativistic hydrodynamics. *International Journal for Numerical Methods in Fluids*, submitted.
5. D'Inverno R. *Introducing Einstein's Relativity*. Oxford University Press: Oxford, 1992.
6. Schutz BF. *A First Course in General Relativity*. Cambridge University Press: Cambridge, MA, 1985.
7. Anile AM. *Relativistic Fluids and Magnetofluids*. Cambridge University Press: Cambridge, MA, 1989.
8. Martí JM, Müller E. The analytical solution of the Riemann problem in relativistic hydrodynamics. *Journal of Fluid Mechanics* 1994; **258**:317–333.
9. Godunov SK. A finite difference method for the computation of discontinuous solutions of the equations of fluid dynamics. *Matematicheskii Sbornik* 1959; **47**:357–393.
10. Martí JM, Müller E. Numerical Hydrodynamics in Special Relativity. *www.livingreviews.org/Articles/Volume2/1999-3marti* 1999.
11. Marquina A, Martí JM, Ibáñez JM, Miralles JA, Donat R. Ultrarelativistic hydrodynamics: high-resolution shock-capturing methods. *Astronomy and Astrophysics* 1992; **258**:566–571.
12. Colella P, Woodward PR. The piecewise parabolic method (PPM) for gas-dynamical simulations. *Journal of Computational Physics* 1984; **54**:174–201.
13. Pons JA, Martí JM, Müller E. The exact solution of the Riemann problem with non-zero tangential velocities in relativistic hydrodynamics. *Journal of Fluid Mechanics* 2000; **422**:125–139.
14. Toro EF. *Riemann Solvers and Numerical Methods for Fluid Dynamics*. Springer: Berlin, 1997.
15. Martí JM, Müller E. Extension of the piecewise parabolic method to one-dimensional relativistic hydrodynamics. *Journal of Computational Physics* 1996; **123**:1–14.
16. Wen L, Panaitescu A, Laguna P. A shock-patching code for ultra-relativistic fluid flows. *Astrophysical Journal* 1997; **486**:919–927.
17. Glimm J. Solution in the large for nonlinear hyperbolic systems of equations. *Communications in Pure and Applied Mathematics* 1965; **18**:697–715.
18. Colella P. Glimm's method for gas dynamics. *SIAM Journal on Scientific and Statistical Computing* 1982; **3**:76–110.
19. Balsara DS. Riemann solver for relativistic hydrodynamics. *Journal of Computational Physics* 1994; **114**: 284–297.
20. Dai W, Woodward PR. An iterative Riemann solver for relativistic hydrodynamics. *SIAM Journal on Scientific Computing* 1997; **18**:982–995.
21. Eulderink F. Numerical relativistic hydrodynamics. *Ph.D. Thesis*, State University of Leiden, 1993.
22. Eulderink F, Mellema G. General relativistic hydrodynamics with a Roe solver. *Astronomy and Astrophysics Suppliment* 1995; **110**:587–623.

23. Roe PL. Approximate Riemann solvers, parameter vectors and difference schemes. *Journal of Computational Physics* 1981; **43**:357–372.
24. Romero JV, Ibáñez JM, Martí JM, Miralles JA. A new spherically symmetric general relativistic hydrodynamical code. *Astrophysical Journal* 1996; **462**:839–854.
25. Yee HC. In *VKI Lecture Notes in Computational Fluid Dynamics*, Von Karman Institute for Fluid Dynamics, Sint Genesius Rode, 1989.
26. Dolezal A, Wong SSM. Relativistic hydrodynamics and essentially non-oscillatory shock capturing schemes. *Journal of Computational Physics* 1995; **120**:266–277.
27. Falle SAEG, Komissarov SS. An upwind numerical scheme for relativistic hydrodynamics with a general equation of state. *Monthly Notices of the Royal Astronomical Society* 1996; **278**:586–602.
28. Harten A, Lax PD, Van Leer B. On upstream differencing and Godunov-type schemes for hyperbolic conservation laws. *SIAM Review* 1983; **25**:35–61.
29. Schneider V, Katscher U, Rischke DH, Waldhauser B, Maruhn JA, Munz CD. New algorithms for ultra-relativistic numerical hydrodynamics. *Journal of Computational Physics* 1993; **105**:92–107.
30. Duncan GC, Hughes PA. Simulations of relativistic extragalactic jets. *Astrophysical Journal* 1994; **436**: L119–L122.
31. Quirk J. A contribution to the great Riemann solver debate. *International Journal for Numerical Methods in Fluids* 1994; **18**:555–574.
32. Donat R, Marquina A. Capturing shock reflections: an improved flux formula. *Journal of Computational Physics* 1996; **125**:42–58.
33. Shu CW, Osher SJ. Efficient implementation of essentially non-oscillatory shock-capturing schemes, 2. *Journal of Computational Physics* 1989; **83**:32–78.
34. Martí JM, Müller E, Font JA, Ibáñez JM. Morphology and dynamics of highly supersonic relativistic jets. *Astrophysical Journal* 1995; **448**:L105–L108.
35. Martí JM, Müller E, Font JA, Ibáñez JM, Marquina A. Morphology and dynamics of relativistic jets. *Astrophysical Journal* 1997; **479**:151–163.
36. Aloy MA, Ibáñez JM, Martí JM, Müller E. GENESIS: A high-resolution code for 3D relativistic hydrodynamics. *Astrophysical Journal Suppliment Series* 1999; **122**:151–166.
37. Davis SF. A simplified TVD finite difference scheme via artificial viscosity. *ICASE Report No.* 84-20, Hampton, VI, 1984.
38. Koide S, Nishikawa KI, Muttel RL. A two-dimensional simulation of a relativistic magnetized jet. *Astrophysical Journal* 1996; **463**:L71–L74.
39. Koide S. A two-dimensional simulation of a relativistic jet bent by an oblique magnetic field. *Astrophysical Journal* 1997; **487**:66–69.
40. Osher S, Solomon F. Upwind difference schemes for hyperbolic conservation laws. *Mathematics of Computation* 1982; **38** (158):339–374.

